Supplementary Figure 1

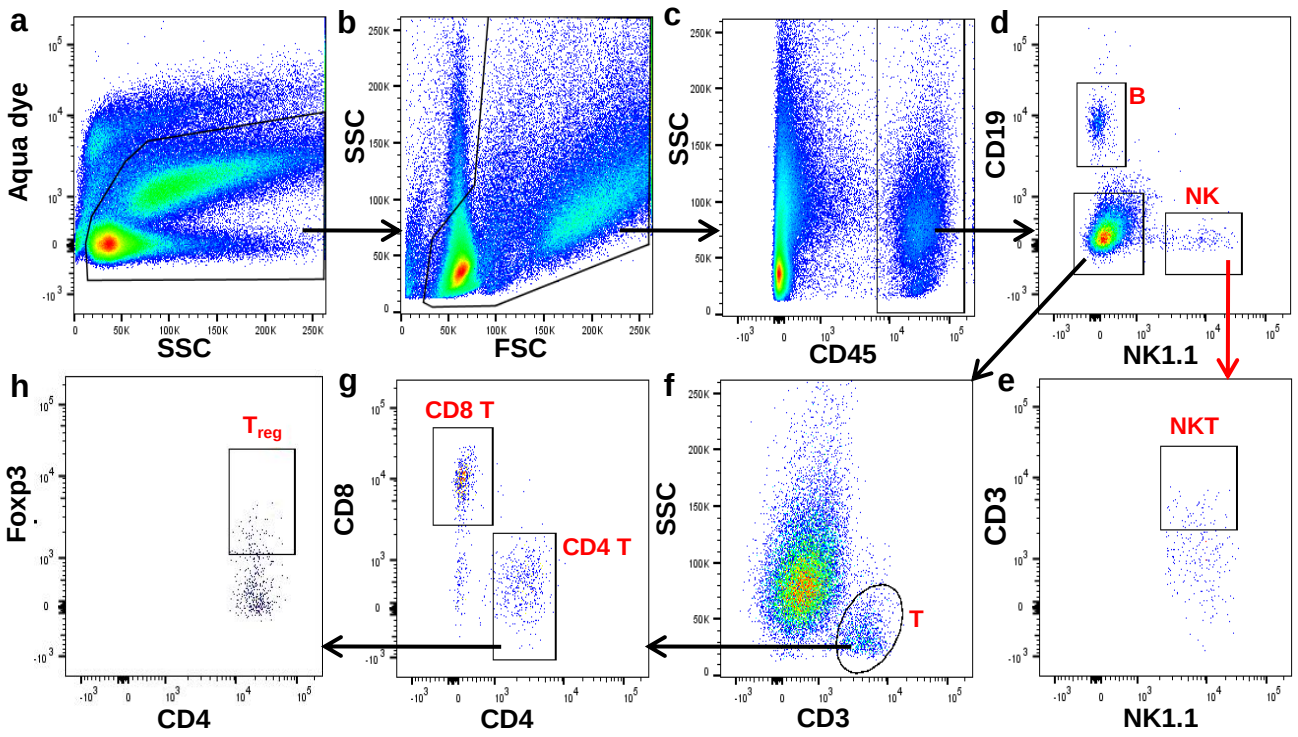

Supplementary Figure 1 Gating strategy used to identify the major lymphocyte populations: B, NK, NKT, CD3⁺ T, CD4⁺ T, CD8⁺ T, and T_{reg} cells. Tumor-containing mouse lung tissues at 13 d p.i. were digested, and cells were stained either with CD45, CD3, CD8, CD4, CD19, and NK1.1 Abs together with Aqua fluorescent reactive dye (dead cell staining) or with CD45, CD3, CD8, CD4, CD19, and Foxp3 Abs together with Aqua fluorescent reactive dye to identify various cell subsets. (**a**) Viable Aqua dye-negative cells were selected; (**b**) Live cells, which were higher up on the forward scatter (FSC) and side scatter (SSC) profile, were then selected; (**c**) $CD45^+$ hematopoietic cells were selected; (**d**) B cells ($CD19^+NK1.1^-$) and NK cells ($CD19^-NK1.1^+$) were identified, and $CD19^-NK1.1^-$ cells and $NK1.1^+$ cells were gated; (**e**) NKT cells ($CD19^-NK1.1^+CD3^+$) were identified; (**f**) T cells ($CD3^+SSC^{low}$) were identified and gated; (**g**) $CD8^+$ T cells ($CD19^-NK1.1^-CD3^+CD4^-CD8^+$) and $CD4^+$ T cells ($CD19^-NK1.1^-CD3^+CD4^+CD8^-$) were identified and (**h**) T_{reg} cells ($CD19^-NK1.1^-CD3^+CD4^+CD8^-Foxp3^+$) were identified among $CD4^+$ T cells. Isotype-matched controls for all Abs were used to determine positive populations. Identified populations are marked in red text.

Supplementary Figure 2

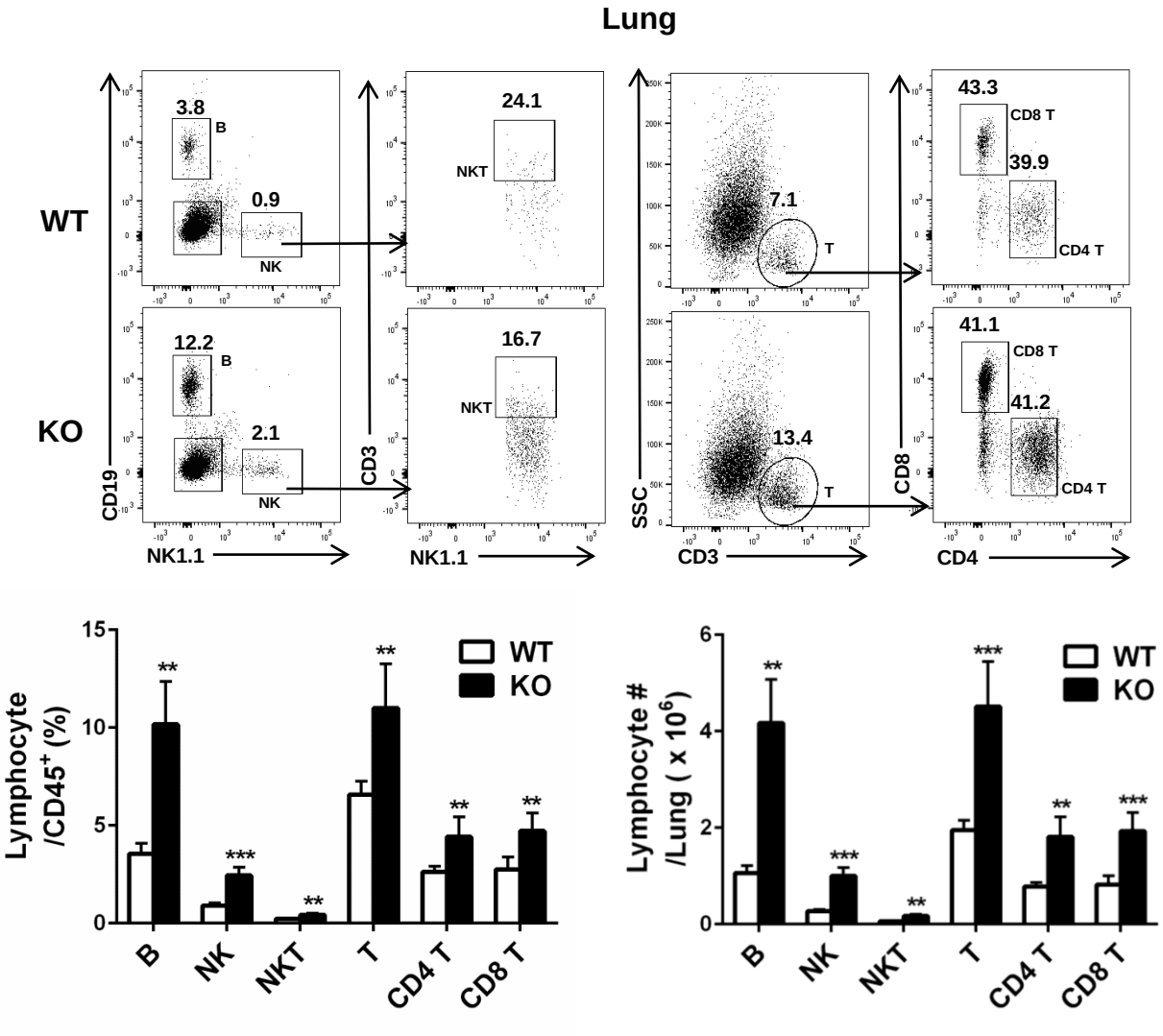

Supplementary Figure 2 TC-1 tumor-challenged *Oasl1*$^{-/-}$ mice contain higher levels of the major lymphocyte populations in their lungs. WT and *Oasl1*$^{-/-}$ (KO) mice (n = 5 per group) were intravenously injected with TC-1 cells (10^6/mice). At 13 d p.i., the left lungs were collected, and the tissue-derived cells were analyzed by FACS. Representative FACS data showing the percentages of B cells ($CD19^+$), NK cells ($NK1.1^+$), and T cells ($CD3^+$) among the $CD45^+$ cells and percentages of NKT ($NK1.1^+CD3^+$) cells, CD4 T cells ($CD3^+CD4^+$), and CD8 T cells ($CD3^+CD8^+$) among the parent population in the lung (top); summary showing lymphocyte subset percentages among the $CD45^+$ cells in the lung (bottom left); summary showing lymphocyte subset numbers in the lung (bottom right). $^{**}p < 0.01$; $^{***}p < 0.001$. Data are representative of at least three independent experiments.

Supplementary Figure 3

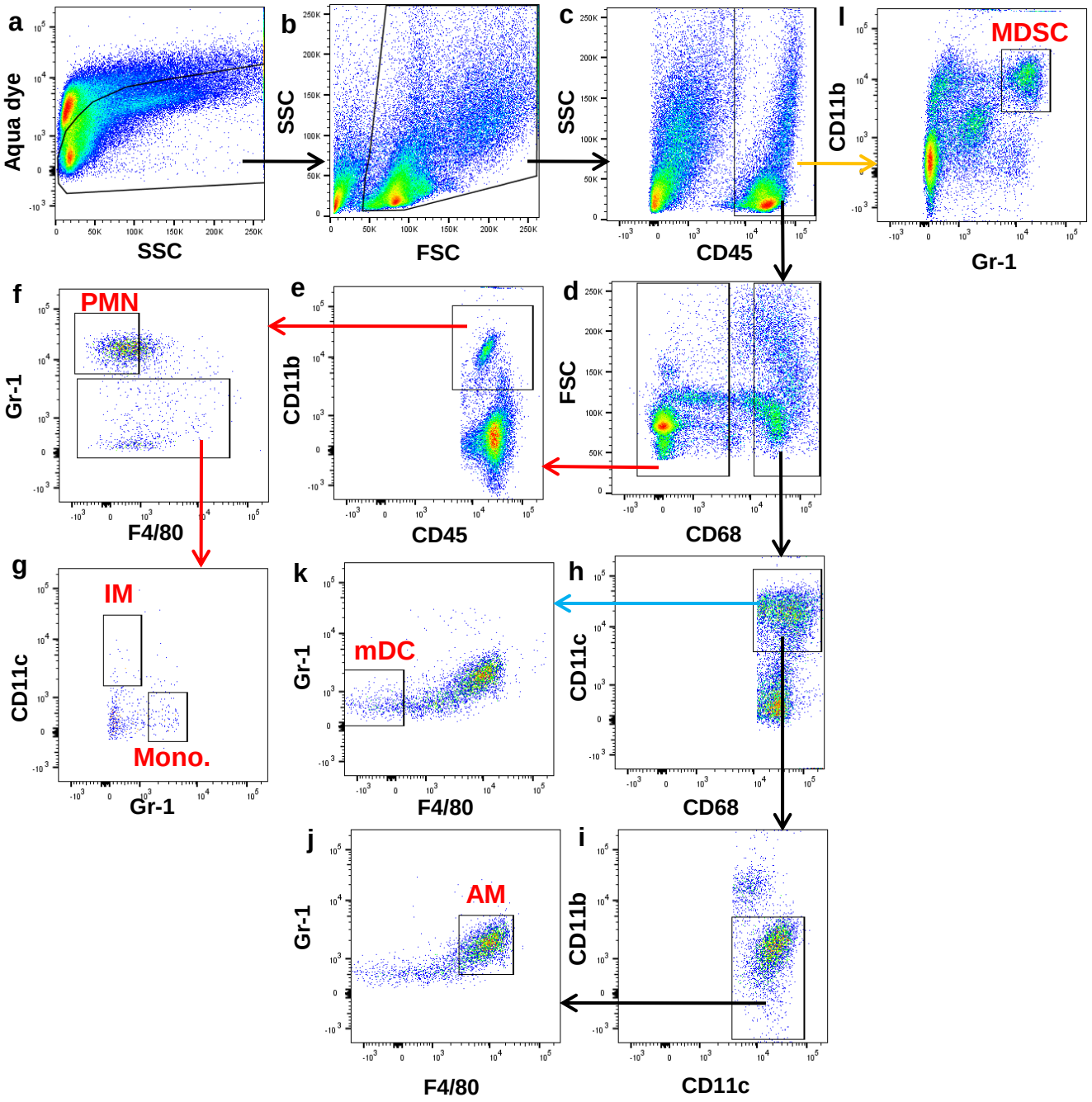

Supplementary Figure 3 Gating strategy used to identify the major pulmonary myeloid populations: PMNs, monocytes (Monos), IMs, AMs, mDCs, and MDSCs from normal mouse lung tissues. This strategy was based on the report by the Rinat Zaynagetdinov group at Vanderbilt University [19]. Lung-derived cells were stained with CD45, CD68, CD11b, F4/80, CD11c, and Gr-1 Abs together with Aqua fluorescent reactive dye (dead cell staining). (**a**) Viable Aqua dye-negative cells were selected; (**b**) Live cells with higher FSC/SSC profiles were then selected; (**c**) $CD45^{+}$ cells were selected; (**d**) $CD68^{hi}$ and $CD68^{low}$ cells were separately gated; (**e**) $CD68^{low}CD11b^{+}$ cells were selected; (**f**) PMN ($CD68^{low}CD11b^{+}F4/80^{-}Gr\text{-}1^{hi}$) were identified, and $CD68^{low}CD11b^{+}Gr\text{-}1^{low}$ cells were gated; (**g**) Monocytes ($CD68^{low}CD11b^{+}Gr\text{-}1^{low}CD11c^{-}$) and IMs ($CD68^{low}CD11b^{+}Gr\text{-}1^{-}CD11c^{+}$) were identified; (**h**) $CD68^{hi}CD11c^{+}$ cells were gated; (**i**) $CD68^{hi}CD11c^{+}CD11b^{-}$ cells were selected; (**j**) AM ($CD68^{hi}CD11c^{+}CD11b^{-}F4/80^{+}Gr\text{-}1^{-}$) were identified; (**k**) mDCs ($CD68^{hi}CD11c^{+}F4/80^{-}Gr\text{-}1^{-}$) were identified, and (**l**) broadly defined MDSCs ($CD11b^{+}Gr\text{-}1^{+}$) were identified. Isotype-matched controls for all Abs were used to determine the positive populations. Identified populations are marked in red text.

Supplementary Figure 4

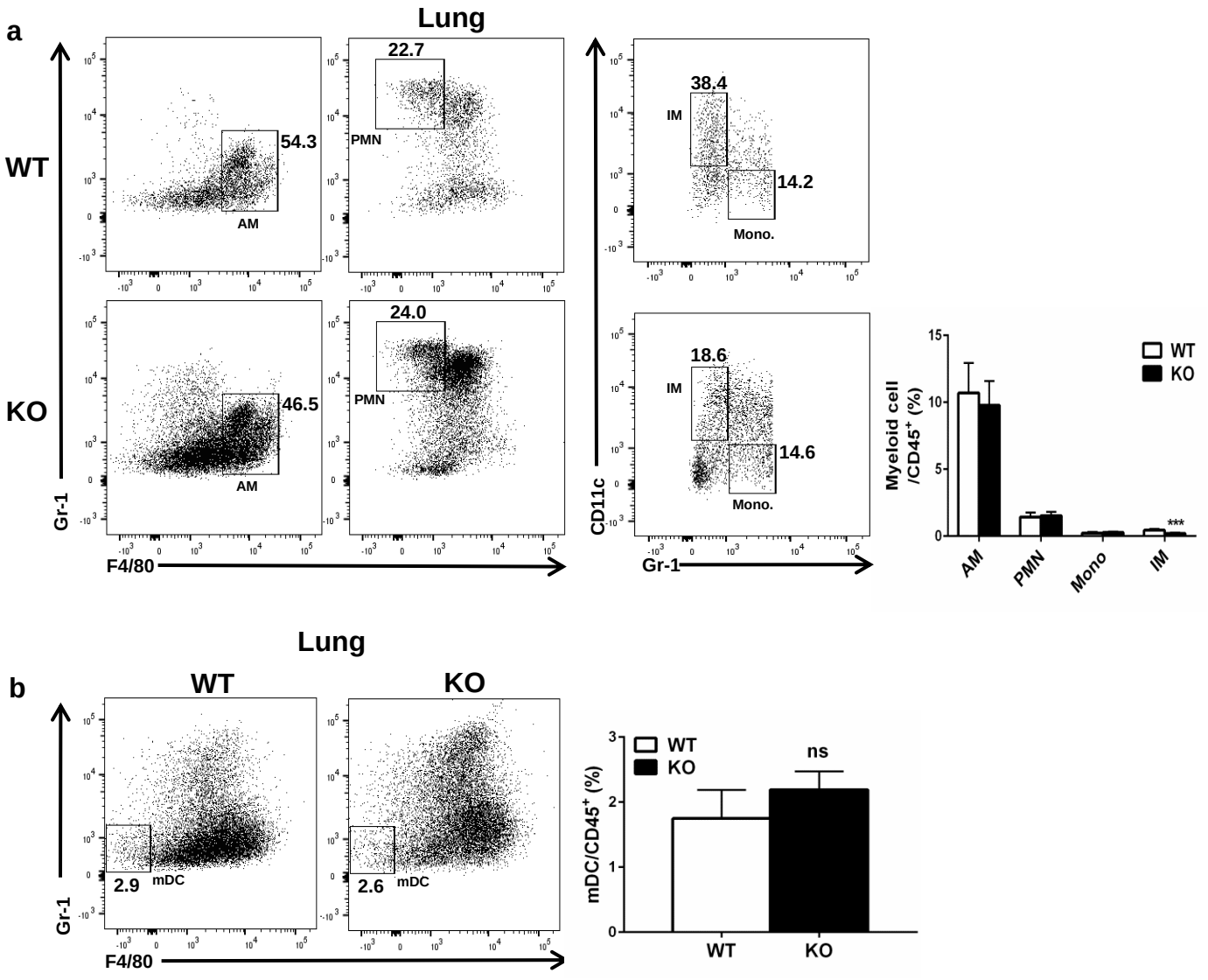

Supplementary Figure 4 TC-1 tumor-challenged *Oasl1*$^{-/-}$ mice contain fewer IMs within the major myeloid cell population analyzed in their lungs. WT and *Oasl1*$^{-/-}$ (KO) mice (n = 5 per group) were intravenously injected with TC-1 cells (10^6/mouse). At 13 d p.i., their left lungs were collected, and the tissue-derived cells were analyzed by FACS. **a-b** Representative FACS data (left) showing the percentages of AMs, PMNs, monocytes (Monos), IMs (**a**), and mDCs (**b**) among the parent populations and a summary (right) showing the percentages of these myeloid cell subsets among the CD45$^+$ cells. ns, not significant; ***p < 0.001. Data are representative of at least three independent experiments.

Supplementary Figure 5

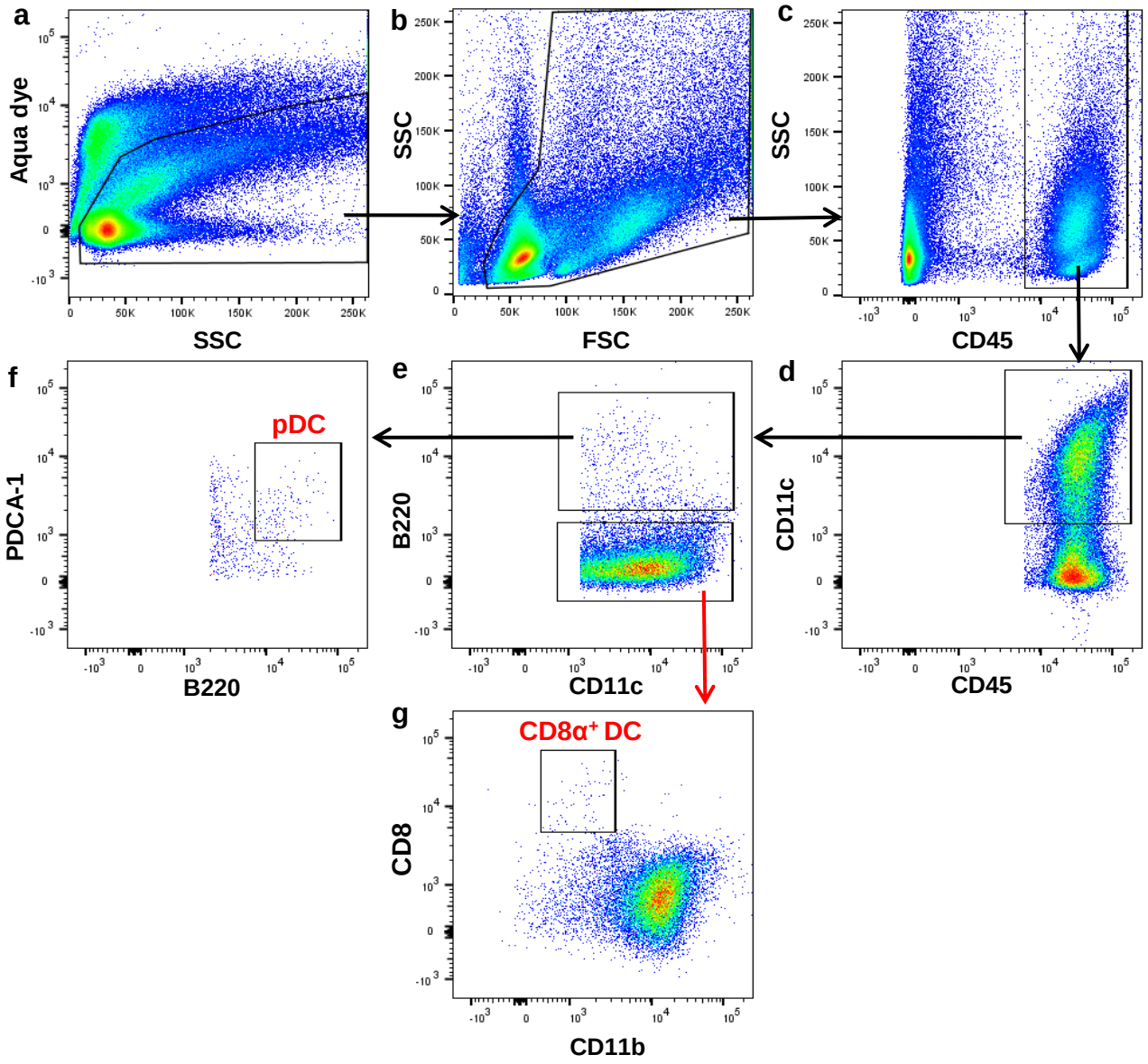

Supplementary Figure 5 Gating strategy used to identify the dendritic cell subsets pDC and CD8α⁺ DC. Tumor-containing mouse lung tissues at 13 d p.i. were digested, and lung-derived cells were stained with CD45, CD11c, B220, CD8, CD11b, and PDCA-1 Abs together with Aqua fluorescent reactive dye (dead cell staining). (**a**) Viable Aqua dye-negative cells were selected; (**b**) Live cells with a higher FSC/SSC profile were then selected; (**c**) $CD45^+$ cells were selected; (**d**) $CD11c^+$ cells were selected; (**e**) $CD11c^+B220^+$ cells were gated, and $CD11c^+B220^-$ cells were separately gated; (**f**) pDC ($CD11c^+B220^+PDCA\text{-}1^+$) cells were identified; (**g**) $CD8\alpha^+$ DC ($CD11c^+B220^-CD8\alpha^+CD11b^-$) cells were identified. Isotype-matched controls for all Abs were used to determine positive populations. Identified populations are marked in red text.

Supplementary Figure 6

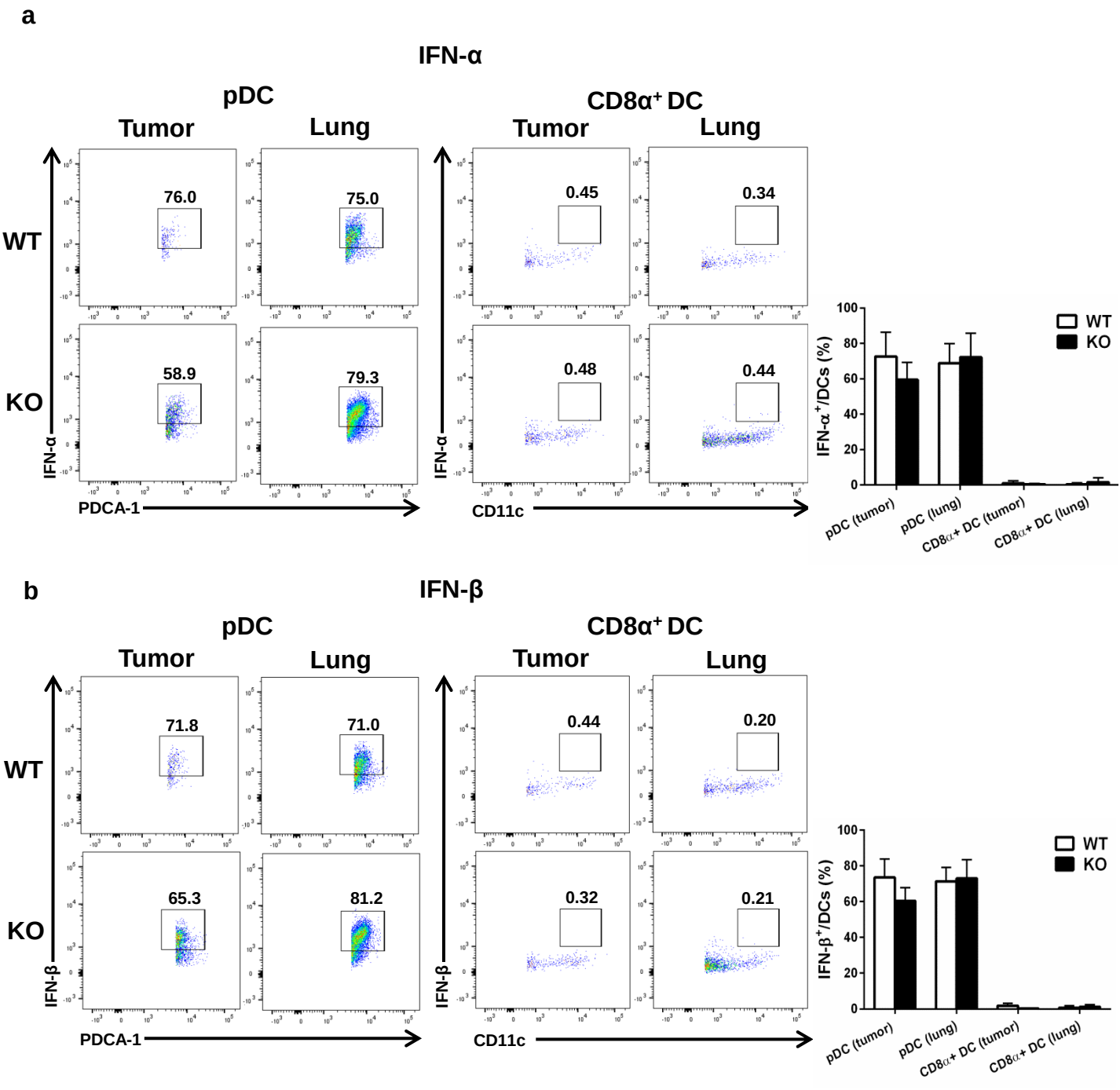

Supplementary Figure 6 pDCs, but not CD8α⁺ DCs, express IFN-Is, IFN-α, and IFN-β in TC-1 tumor-challenged WT and *Oasl1*$^{-/-}$ mice. WT and *Oasl1*$^{-/-}$ (KO) mice (n = 5 per group) were intravenously injected with TC-1 cells (10^6/mice). At 13 d p.i., their growing tumors (same size) in the right lungs (tumor samples) and the entire left lungs (lung samples) were collected, and the tissue-derived single cells were analyzed by FACS. Representative FACS data (left and middle) showing the percentages of (**a**) IFN-α- and (**b**) IFN-β-producing pDCs and CD8α⁺ DCs in the tumors and lungs and a summary (right) showing the percentages of IFN-I-producing pDCs and CD8α⁺ DCs. Data are representative of at least two independent experiments.

Supplementary Figure 7

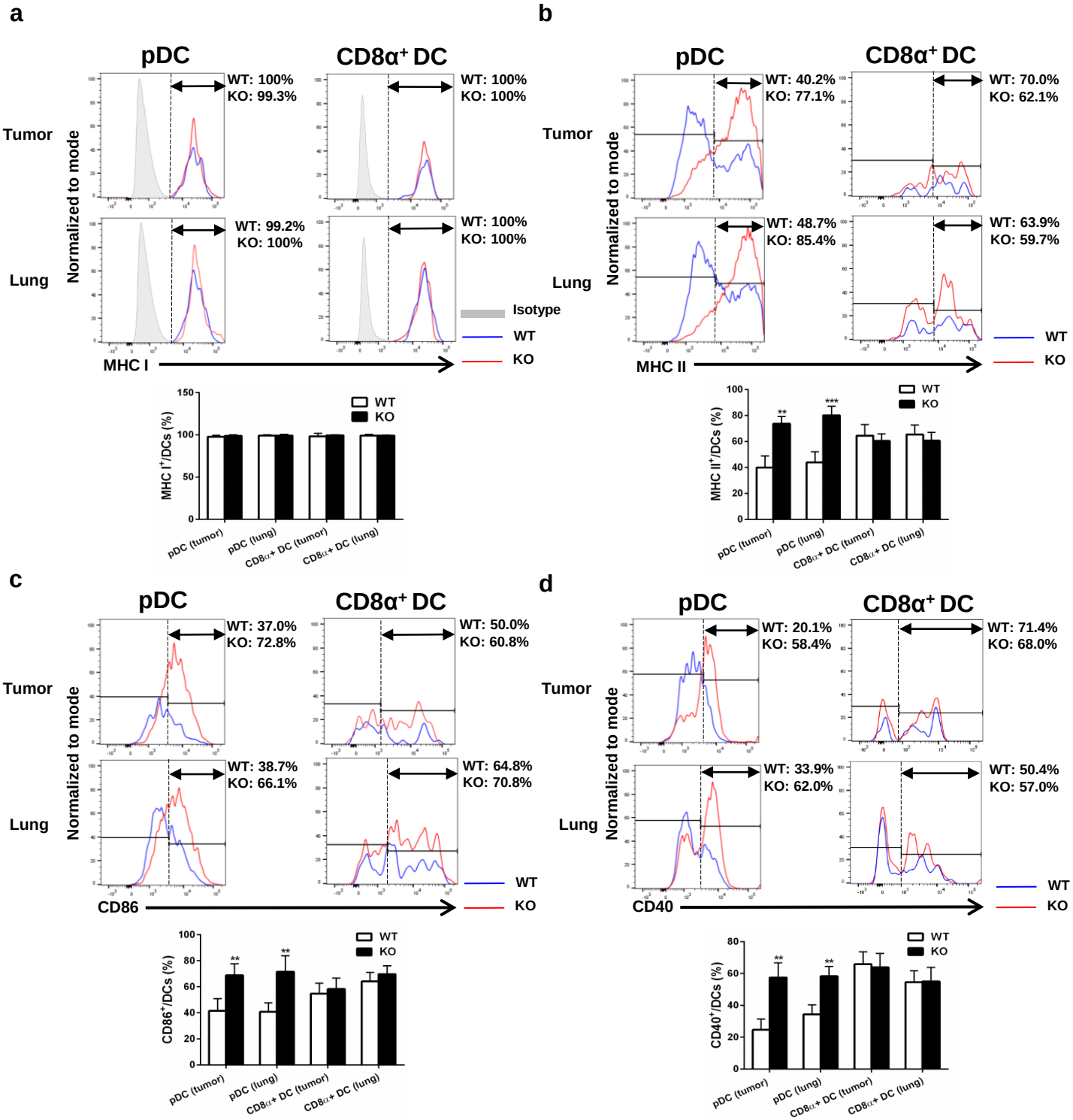

Supplementary Figure 7 Large proportions of pDCs and CD8α⁺ DCs express DC maturation markers in the tumors and lungs of TC-1 tumor-challenged WT and *Oasl1*$^{-/-}$ (KO) mice, with a higher proportion of pDCs expressing such markers in *Oasl1*$^{-/-}$ mice. WT and *Oasl1*$^{-/-}$ (KO) mice (n = 5 per group) were intravenously injected with TC-1 cells (10^6/mouse). At 13 d p.i., their growing tumors (same size) in the right lungs (tumor samples) and the entire left lungs (lung samples) were collected, and the tissue-derived single cells were analyzed by FACS. Representative FACS data (upper in each panel) showing the percentages of cells expressing (**a**) MHC I, (**b**) MHC II, (**c**) CD86, or (**d**) CD40 among each DC subset and a summary (lower in each panel) showing these percentages in each DC subset. $^{**}p < 0.01$; $^{***}p < 0.001$. Data are representative of at least two independent experiments.

Supplementary Figure 8

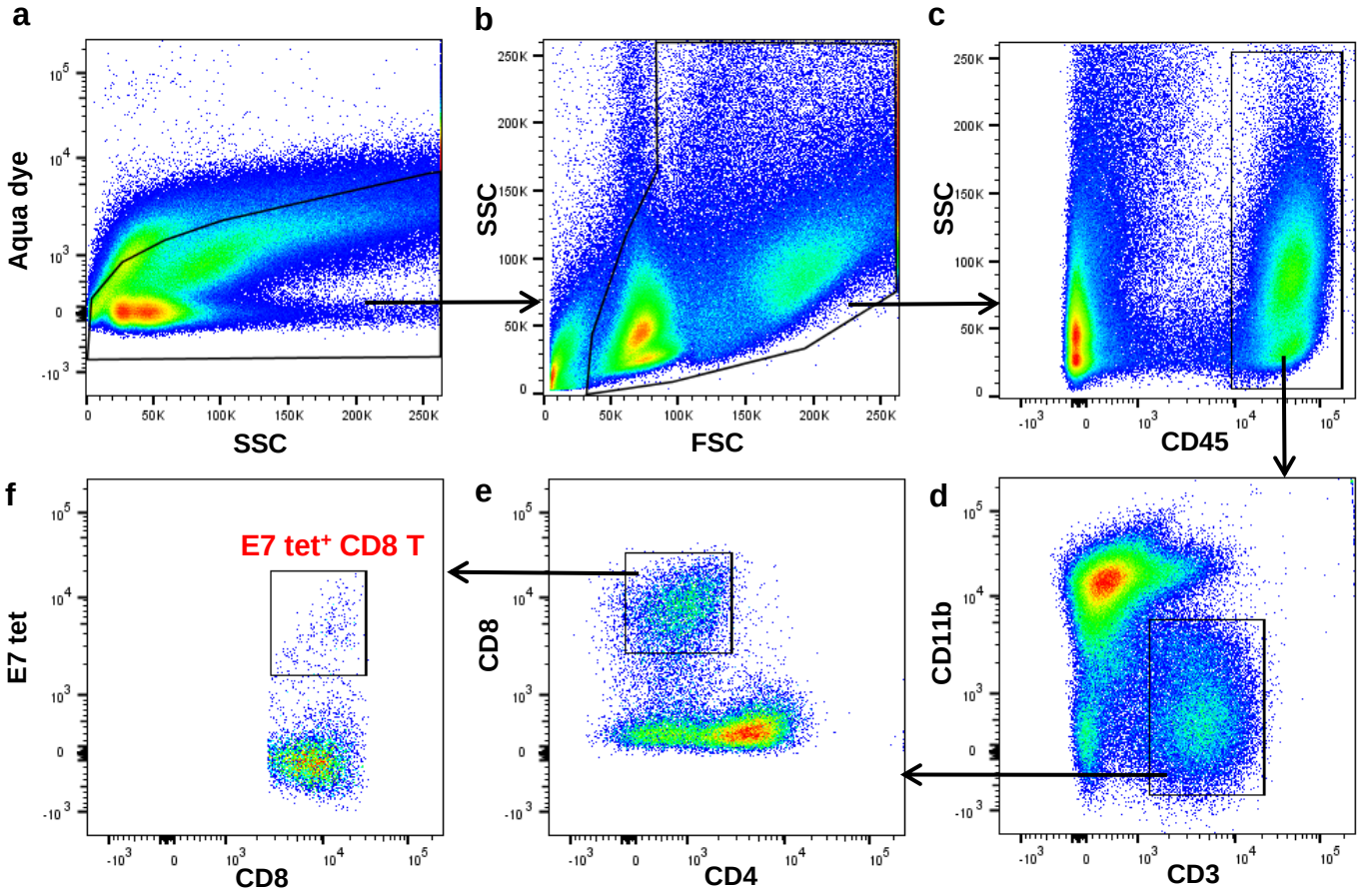

Supplementary Figure 8 Gating strategy used to identify tumor antigen (E7)-specific CD8⁺ T cells. Tumor-containing mouse lung tissues were digested, and lung-derived single cells were stained with CD45, CD11b, CD3, CD4, and CD8 Abs; E7-specific tetramer (E7 tet); and Aqua fluorescent reactive dye (dead cell staining). (**a**) Viable Aqua dye-negative cells were selected; (**b**) Live cells with a higher FSC/SSC profile were then selected; (**c**) $CD45^+$ cells were selected; (**d**) $CD3^+CD11b^-$ cells were gated; (**e**) $CD8^+$ T ($CD3^+CD4^-CD8^+$) cells were selected; (**f**) E7-specific $CD8^+$ T ($CD3^+CD4^-CD8^+Tet^+$) cells were identified. Isotype-matched controls for all Abs were used to determine the positive populations. Identified populations are marked in red text.

Supplementary Figure 9

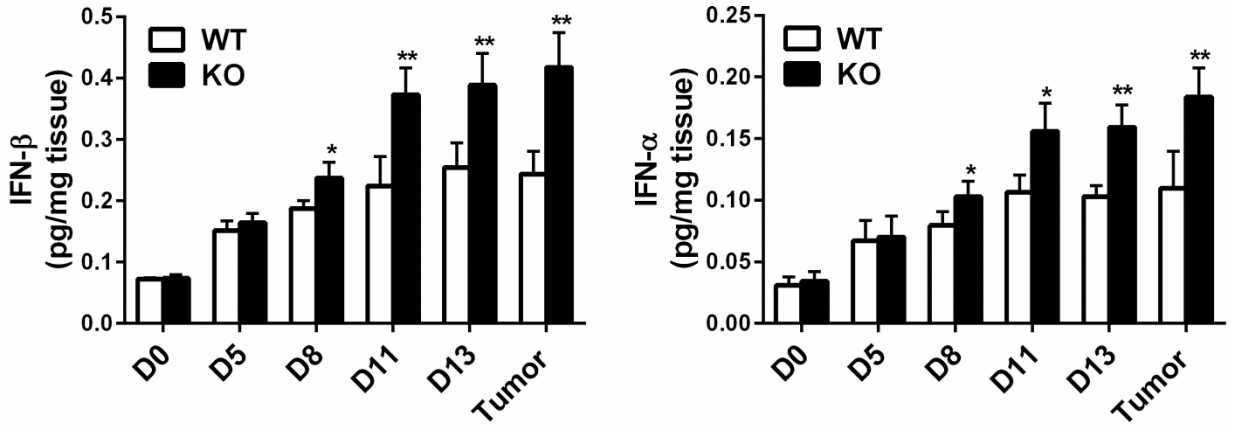

Supplementary Figure 9 TC-1 tumor-challenged *Oasl1*$^{-/-}$ mice produce more IFN-I proteins (IFN-α and IFN-β) in their tumors. WT and *Oasl1*$^{-/-}$ (KO) mice were intravenously injected with TC-1 cells (10^6/mice), and their lungs at the indicated d p.i. (D0, D5, D8, D11, and D13) and tumors (at 13 d p.i.) were collected. IFN-I protein levels (IFN-α and IFN-β) were measured by ELISA. IFN-I protein quantity (pg) per tissue amount (mg) is shown. *$p < 0.05$; **$p < 0.01$. Data are representative of at least three independent experiments.

Supplementary Figure 10

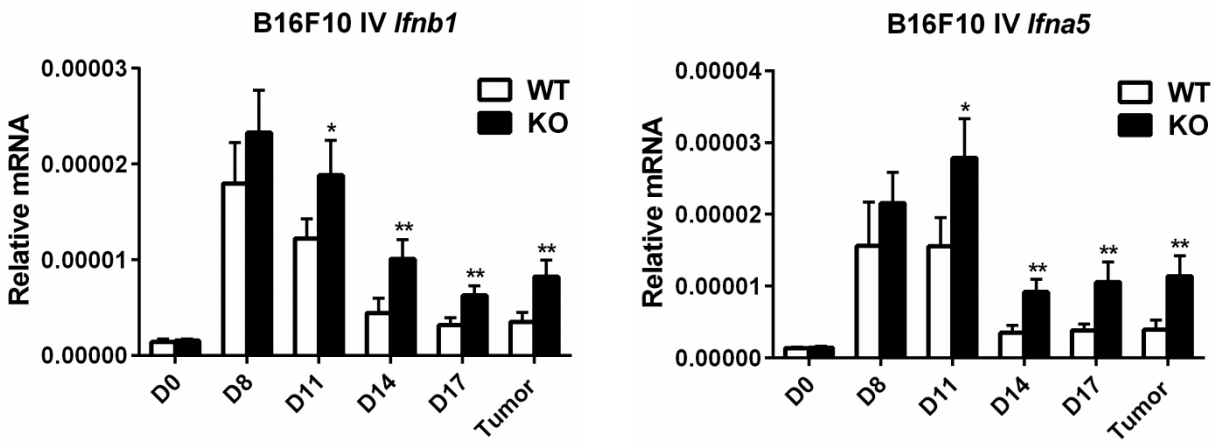

Supplementary Figure 10 B16F10 tumor-challenged *Oasl1*$^{-/-}$ mice express more IFN-I mRNA in their tumors. WT and *Oasl1*$^{-/-}$ (KO) mice were intravenously injected with B16F10 cells (10^6/mice), and their lungs at the indicated d p.i. (D0, D8, D11, D14, and D17) and tumors (at 17 d p.i.) were collected for RNA analysis. Quantitative RT-PCR analysis of mRNA expression levels of *Ifnb1* and *Ifna5* was performed. mRNA expression level (n = 4 per group) normalized to that of *Gapdh* is shown as relative mRNA. *$p < 0.05$; **$p < 0.01$. Data are representative of at least two independent experiments.

Supplementary Figure 11

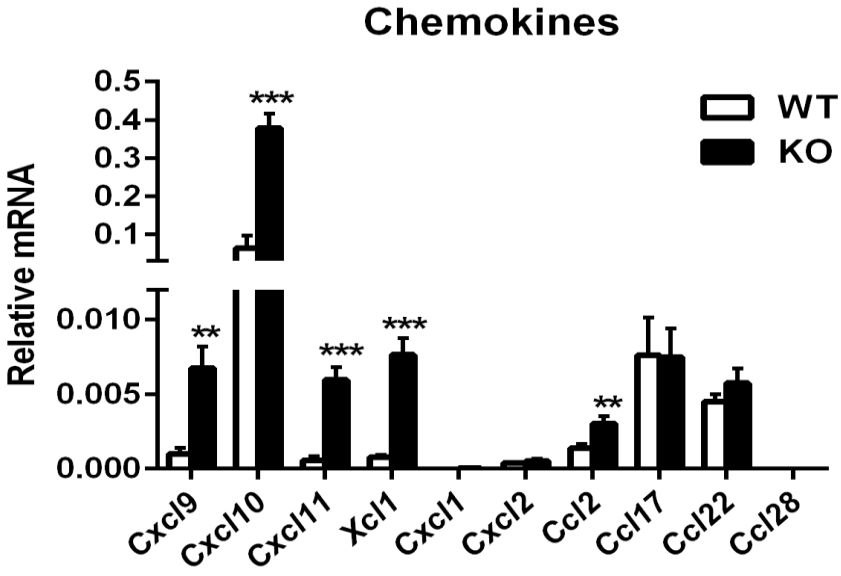

Supplementary Figure 11 Expression patterns for the major chemokines that recruit immune cells to tumor sites of TC-1 tumor-challenged mice. WT and *Oasl1*$^{-/-}$ (KO) mice were intravenously injected with TC-1 cells (10^6/mice), and their lung tumors at 13 d p.i. were collected for RNA analysis. Quantitative RT-PCR analysis of the mRNA expression level of each chemokine gene was performed using the following gene-specific forward (F) and reverse (R) primers: *Gapdh* F: GGCAAATTCAACGGCACAGTCAAG and R: TCGCTCCTGGAAGATGGTGATGG; *Cxcl9* F: ACATCAGGCTAGGAGTGGTG and R: CACAAGGCTCACGCACAC; *Cxcl10* F: CATGAACCCAAGTGCTGCCGTCA and R: TGGATGCAGTTGCAGCGGACCGT; *Cxcl11* F: ATCTGGGCCACAGCTGCTCAAG and R: CTCGATCTCTGCCATTTTGACGGCTT; *Xcl1* F: GAAGAGAGTAGCTGTGTGAACTTACAAAC and R: CCCATTTGGCTTCTGGATCAGCACA; *Cxcl1* F: CTGCGCTGTCAGTGCCTGCA and R: GCAGTCTGTCTTCTTTCTCCGTTACTTG; *Cxcl2* F: GGGTTGACTTCAAGAACATCCAGAGCT and R: CTCCTTTCCAGGTCAGTTAGCCTTG; *Ccl2* F: AGAGCTACAAGAGGATCACCAGCA and R: GAAGACCTTAGGGCAGATGCAGT; *Ccl17* F: GTACCATGAGGTCACTTCAGATGCTG and R: GAAGTAATCCAGGCAGCACTCTCG; *Ccl22* F: TCCGTCACCCTCTGCCATCAC and R: TGGGATCGGCACAGATATCTCGGTT; and *Ccl28* F: CATGCAGCATCCAGAGAGCTGAC and R: TCTGAGGCTCTCATCCACTGCTTC. mRNA expression level (n = 4 per group) normalized to that of *Gapdh* is shown as relative mRNA. $^{**}p < 0.01$; $^{***}p < 0.001$. Data are representative of at least two independent experiments.